Vibration Suppression of the Friction Plate Based on the Gear Tooth Profile Modification for a Six-Speed Planetary Gear Transmission System

Yan Cheng

Department of Automotive Engineering, School of Transportation Science and Engineering, Beihang University, Beijing 100191, PR China.
Key Laboratory of Vehicle Transmission, China North Vehicle Research Institute, Beijing 100072, PR China.

Yanfang Liu

Department of Automotive Engineering, School of Transportation Science and Engineering, Beihang University, Beijing 100191, PR China. E-mail: artibuaa@163.com

Hongwu Li

Key Laboratory of Vehicle Transmission, China North Vehicle Research Institute, Beijing 100072, PR China.

(Received 2 December 2024; accepted 23 June 2025)

Friction plates are critical parts of clutch operators for the planetary gear transmission system (PGTS). Their healthy working conditions have significant importance on the steady operations of the PTGS. However, continuous impact could occur between the friction plates and inner hub of clutches, which have great influences on the stability and lifetime of friction plates. In this paper, the multibody dynamic model of a six-speed planetary gear transmission system (SSPGS) is proposed. The impact forces between the friction plates and inner hubs are calculated based on multibody theory. The gear tooth tip modifications are introduced and the meshing forces between gear pairs are calculated and considered. The SSPGS model is simulated and the vibration characteristics of the inner hubs under different tooth modification amounts are obtained and compared. The effectiveness of the tooth tip modification on the vibration mitigation of the SSPGS is investigated. Several suggestions for the design of the high stable SSPGS are provided.

1. INTRODUCTION

For the advantages of compact structure and high gear ratio, the planetary gear systems (PGS) are widely applied as the power transmission systems of various vehicles powertrains. Friction plates are key components of the PGS clutch operators and their working conditions can be crucial for the stableness of gear switching for the PGS. Previous research indicates that the impact loads between the friction plates and inner hubs of the clutches are the main causes of damage to friction plates. Thus, studying the vibration characteristics and the mitigation methods of inner hub can be beneficial to the design of high stable PGS.

Many researchers have proposed the impact model of the friction plates and inner hubs. Zhang et al.[1] proposed an original dynamic impact model. They investigated the influences of backlash, impact position on the impact characteristic of meshing teeth between friction plate and the inner hub of the clutch. Chen et al.[2] established the multibody dynamic model of a six-speed planetary gear transmission system (SSPGS). They studied the dynamic contact forces between the friction plates and inner hub. Li et al.[3] improved the previous model to both consider the influences of radial clearance and backlash. They investigated the effects of the two factors on the vibrations and impact forces of friction plate. Liu et al.[4] proposed the impact model of the Ravigneaux planetary gear set with two ring gears based on the finite element method. They investigated the stress distribution of the floating friction plate. Pan et al.[5] developed the dynamic model of a hydraulic disk brake with floating friction plate. They studied the dynamic contact forces characteristic result from time-varying clearances. Zhu et al.[6] established the dynamic and temperature-filed model of the dry friction clutch for an aircraft. They studied the effects of engagement control on the mitigation of impact torque. Zhang et al.[7] proposed the dynamic contact impact model of the friction pairs of the multiplate wet clutch. They revealed the nonlinear motion and impact characteristic of the friction pair. Yang et al.[8] established the lateral motion equations of the rotating circular friction plate. They studied the transverse vibration and provided optimized structure of the clutch friction plate. Qu et al.[9] proposed the dynamic model of an automobile powertrain. They investigated the clutch parameters on the tortional vibration of the system. Bao et al.[10] established the bending torsional dynamic model of the gear transmission system. They studied the joint state on the radial vibration of the clutch. Ning et al.[11] provided an improved friction plate structure with damping materials to suppress the dynamic load. They simulated the damping holes positions and numbers on the effec-

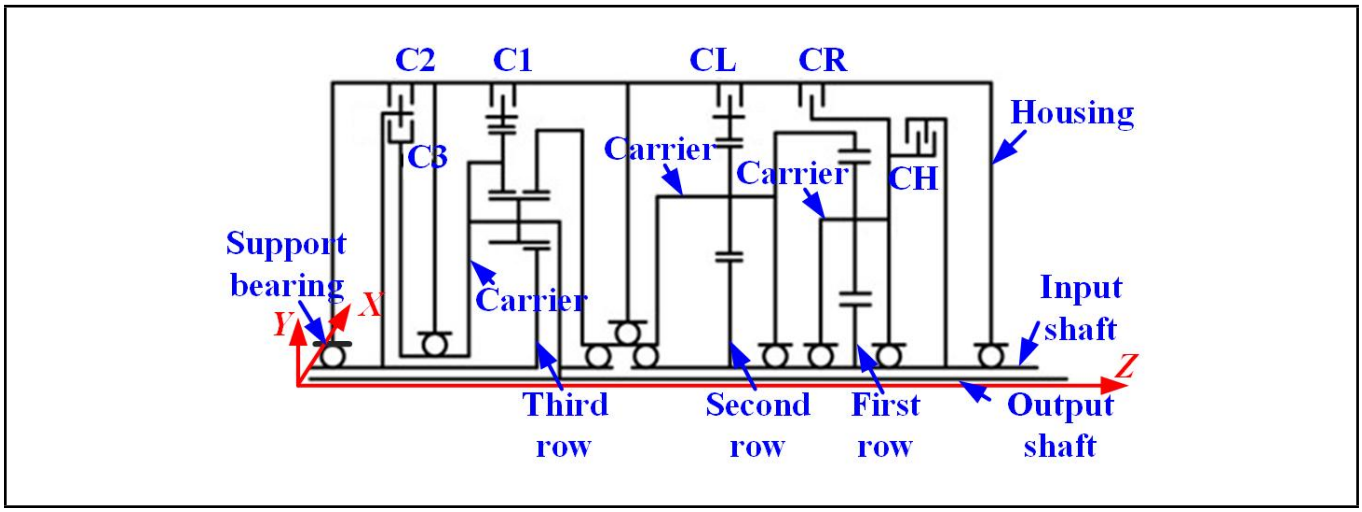

Figure 1. Schematic of the six-speed planetary gear transmission system.

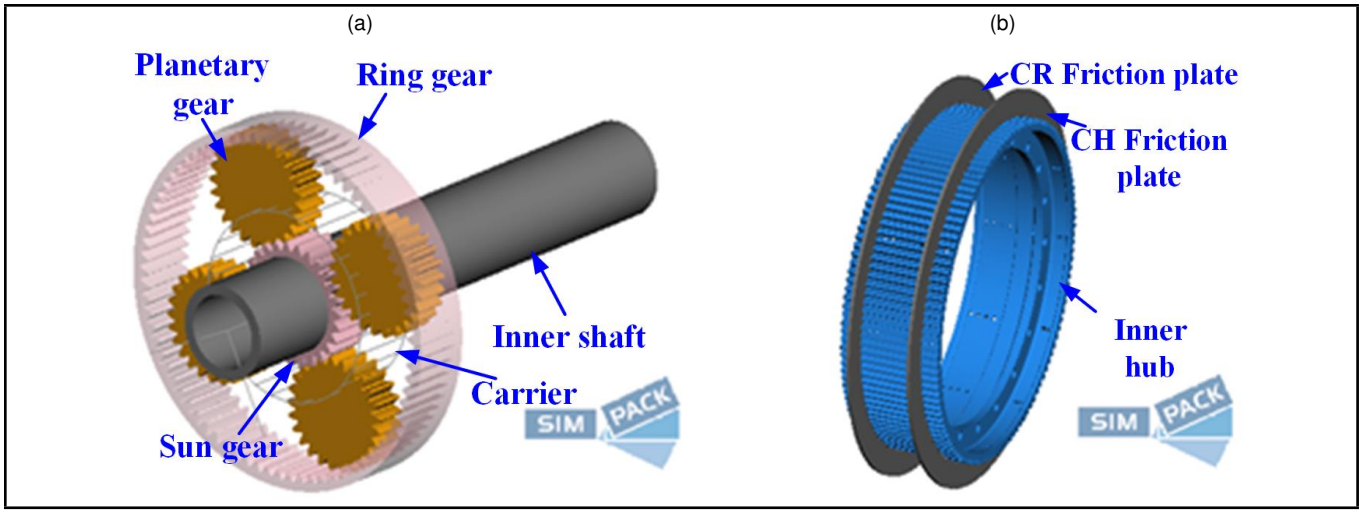

Figure 2. Three-dimensional model of the first-row planetary gears. (a) Gears, (b) CH, CR friction plates and inner hubs.

tiveness of dynamic load mitigation.

Some researchers have studied the effects of tooth profile modification on the vibration mitigation of gear systems. Öztürk et al.[12] proposed the dynamic model of the PGS. They revealed the relationships between the tooth profile modification and the dynamic characteristics of the PGS by performing parametric studies. Liu et al.[13] proposed the multibody dynamic model of a double-row PGS supported by planet bearings. They investigated the roller profile modification on the vibration mitigation of the gear system. Liu and Li et al.[14–16] established the flexible shaft gear transmission system dynamic model. They investigated the tooth profile modification on the vibration characteristic of the flexible gear system. Gao et al.[17] established the lateral torsional coupling model of the gear system. They optimized a modification method for the dynamic load reduction of the spur gear system. Huangfu et al.[18] put both the thin rim structure and tooth modification into consideration. They developed the wear prediction model of the gear system. They found that tooth profile modification can benefit the dynamic load and wear distribution on gear surfaces. Xu et al.[19] proposed the gear tooth modification model of the PGS. They found that the tooth modification can significantly reduce the dynamic load while not markedly change the meshing stiffness of gear pairs.

The literature review highlights that the impact models are mainly including the friction plates and inner hubs of clutches. The whole dynamic model including the friction plates, inner hubs and the PGS are rarely proposed. Moreover, the effectiveness of gear tooth modification on the impact between friction plates and inner hubs are rarely investigated. To fill this gap, a multibody dynamic model of the SSPGS is established based on multibody theory. The dynamic model of the SSPGS is calculated and the inner hub of maximum vibration is located. The tip modification is introduced to suppress the vibration of inner hub and the effects of gear tooth modification on the vibrations of inner hub are investigated.

2. DYNAMIC MODEL OF THE SIX-SPEED PLANETARY GEAR TRANSMISSION SYSTEM

2.1. Structures of the SSPGS

The structure of a six-speed planetary gear transmission system (SSPGS) is shown in Fig. 1. The SSPGS housing was supposed to be fixed and the components including sun gears,

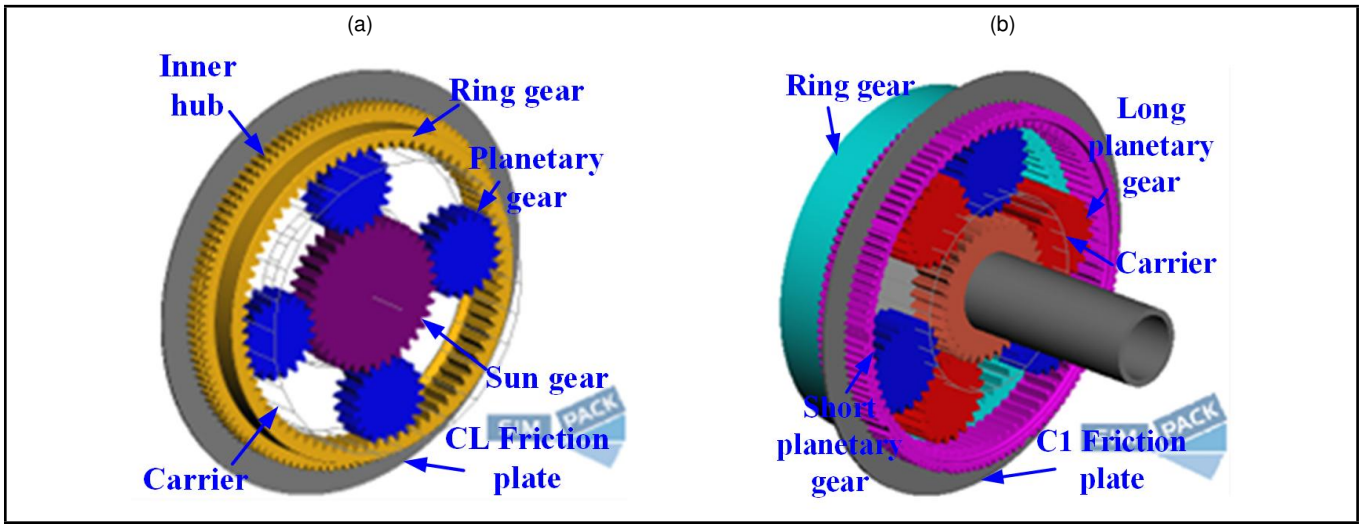

Figure 3. Three-dimensional model of the (a) Second-row planetary gears, (b) Third-row planetary gears.

planetary gears and ring gears of SSPGS are engaged and supported by the bearings. Depending on the proximity of the planetary gear rows to the input shaft, the planetary rows were named as first row, second row, and third row. There were six clutches for SSPGS and they were named as CH, CR, CL, C1, C2 and C3 in sequence. By operating different clutches, the SSPGS can switch six speed ratios. According to the components' dimensions and connections, the multi-body dynamic model of the SSPGS was established using Simpack software.

The three-dimensional model of the first-row planetary gears are shown in Fig. 2. For the first row, the sun gear was engaged with four planetary gears, and the friction plates of clutches CH and CR were engaged with the same inner hub. Unlike the first row, the inner hub and ring gear of second-row planetary gears were fixed connected, as shown in Fig. 3(a). As shown in Fig. 3(b), the structure of the third-row planetary gears was more complicated, the sun gear was engaged with three long planetary gears, then the long planetary gears were engaged with each short planetary gear. The inner ring and the inner hub are fixed connected and the friction plate of clutch C1 is engaged with the inner hub.

2.2. Kinematic Modeling of the SSPGS

In the Simpack simulation conditions, there were kinds of joints can be used to restrict the motions of SSPGS components. The joint #0: 0 Degree of Freedom can restrict all the degrees of freedom (DOFs) of the object and can be used to connect the two components of same motion state The object with joint #22: Planar ga-x-y can only revolute around Z axis and move along X and Y axes. For the SSPGS depicted in Fig. 1, the usage of the #0 and #22 joints on the components are shown in Tables 1 and 2.

The model was established under the following assumptions: (1) All gear components in the SSPGS multibody dynamic model were treated as rigid bodies with flexible deformations neglected; (2) influences of the tooth profile modifications on their load-carrying capacity were excluded from the analysis; (3) tooth surface wear during gear meshing processes was disregarded.

Table 1. Usage of the #0 joint.

From component	To component
Land	Housing
Input shaft	Sun gears of the first-row and second-row Outer hub of the clutch CH
Carrier of the first-row	Inner hub of the clutches CH and CR
Ring gear of the first-row	Carrier of the second-row
Ring gear of the second-row	Inner hub of the clutch CL
Carrier of the second-row	Ring gear engaged with the long planetary gear of the third-row
Ring gear engaged with the short planetary gear of the third-row	Inner hub of the clutch C1
Carrier of the third-row	Inner hub of the clutch C3 Output shaft
Sun gear of the third-row	Outer hub of the clutch C3 Inner hub of the clutch C2

Table 2. Usage of the #22 joint.

From component	To component
Housing	Input shaft Carrier of the first-row Ring gear of the first-row Carrier of the third-row Friction plates of clutches CH, CR, CL, C1, C2 and C3
Carrier of the first-row	Planetary gears of the first-row
Carrier of the second-row	Planetary gears of the second-row
Carrier of the third-row	Long planetary gears of the third-row Short planetary gears of the third-row

The motion states for the components of the SSPGS can be specified and the kinetic model is established. By operating clutches, the six forward gears (F1 to F6) and two reverse gears (R1 and R2) can be shifted. The specific clutch operation for each gear of SSPGS is shown in Table 3. In the SSPGS multi dynamic model, the joint #0 is utilized to simulate the operation of the clutches. In this study, the transmission ratios of the SSPGS from gear F1 to R2 were 8.403, 5.558, 3.652, 2.301, 1.522, 1, −5.969 and −4.191.

Table 3. Usage of the #0 joint for each forward and reverse gear.

Gear	From component	To component
F1	CL C1	Housing Housing
F2	CL C2	Housing Housing
F3	CL Carrier of the third-row	Housing Sun gear of the third-row
F4	CH C1	Carrier of the first-row and input shaft Housing
F5	CH C2	Carrier of the first-row and input shaft Housing
F6	CH C3	Carrier of the first-row and input shaft Inner hub of C2
R1	CR C1	Housing Housing
R2	CR C2	Housing Housing

2.3. Contact Forces Between Components of the SSPGS

The gear meshing forces between the engaged gear pairs were described by force element #225: Gear Pair. The gear meshing forces were normal to the contact surfaces of gears and depend on the penetration depth of the undeformed teeth profiles and on the contact stiffnesses. The normal contact stiffness of each tooth pair followed a parabolic function and its highest value is reached at the pitch point

$$c(\varphi) = c_{\max}\left(1-(1-S_R)\left(\frac{s(\varphi)}{\max(s_{1c},s_{2c})}\right)^2\right); \quad (1)$$

$$c_{\max} = \frac{\pi EL}{4(1-\nu^2)}; \quad (2)$$

where φ represented the angular position; $c_{\max}$ represented the highest value of Hertzian contact stiffness;[20–22] L represented the tooth width; E and ν represented the modulus of elasticity and the Poisson ratio; S_R was the stiffness ratio, which was set as 0.8;[14] s_{1c} and s_{2c} were the distances from the pitch point to the two points along the contact path.

In industry, the gear profile modification has been widely used to the mitigation of load and vibration of gear system. The modification amount generally ranges from 5 μm to 25 μm and which is also depending on the dimensions of gears. In this SSPGS multi dynamic model, the tip modification was applied on the gear components. The schematic of the gear tip modification is shown in Fig. 4. As depicted in Fig. 4, the r_{Ca} was the distance of the modification end point to the gear geometry center, Ca was the modification amount. Moreover, the profiles of gear surfaces were changing accordingly with the exponent Pa. Generally, the second order profile modification are most popular.

The force element #197: Geo.Prim.Contact was utilized to describe the dynamic contact forces between friction plates and the inner hub of clutches. As shown in Fig. 5, the relative penetration depths of components can be calculated by the distances between 'From Marker' and 'To Marker' on the components. If the penetration depth was greater than zero, it means the two objects were not in contact; if the penetration depth was less than zero, it indicated that the two objects were in contact. The contact forces between friction plates and the inner hub of clutches can then be calculated based on the penetration depths and Hertzian contact stiffnesses.

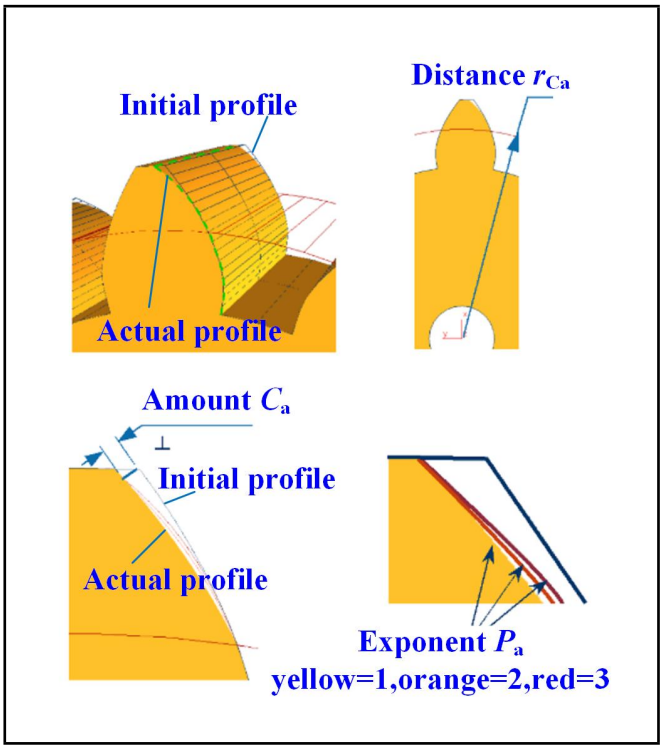

Figure 4. Schematic of the gear tip modification.

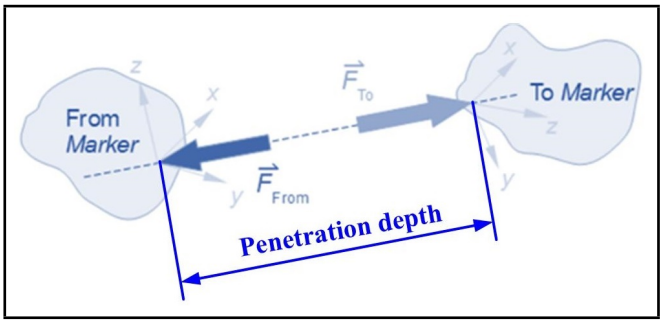

Figure 5. Calculation of penetration depth between contact components.

To more clearly demonstrate the modeling process and computational procedures of the SSPGS dynamic model, the modeling workflow is illustrated in Fig. 6. First, establish geometric models of SSPGS gear components based on parameters such as gear geometric dimensions and mass; subsequently, define joints according to kinematic relationships between components; then, specify contact forces for meshing gear pairs; finally, complete the establishment of the SSPGS multibody dynamic model.

3. EXPERIMENTAL VALIDATION

To verify the correction of the proposed dynamic model, a rest rig of the studied six-speed planetary gear transmission system was established, as depicted in Fig. 6. During operation, the ring gear was floating and can bring great challenges for vibration testing. To address the problem, a specialized collector including sensor module, conditioning circuit, central processing module, storage module, power supply module was

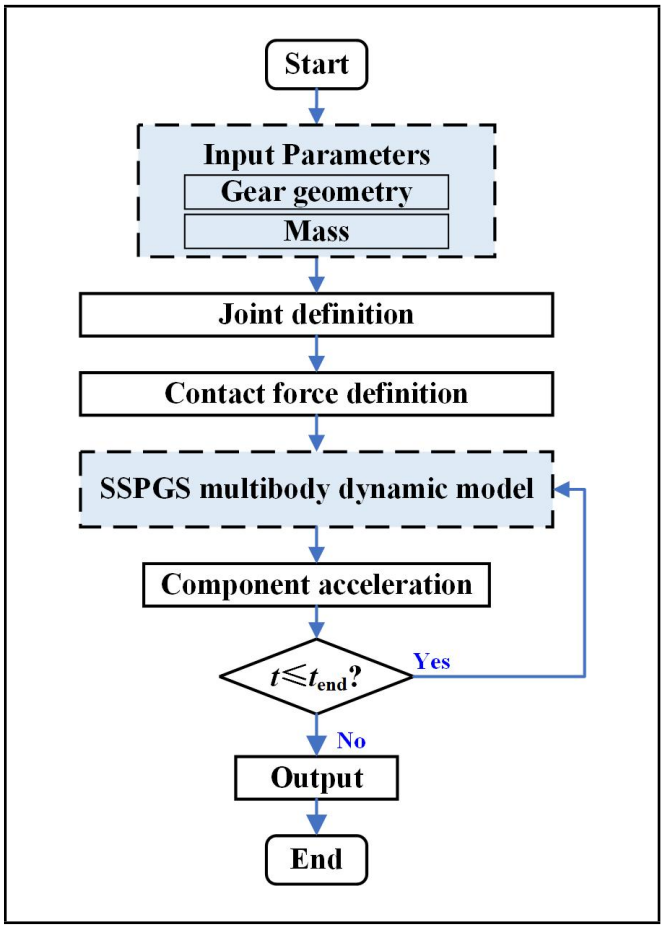

Figure 6. Simulation process of the SSPGS dynamic model.

designed. There were four MEMS accelerometers ADXL1001 uniformly arranged on the collector. The sensitivity of the accelerometer was 10 mv/g (power supply 5 V), the measuring range was ± 100 g. The four MEMS accelerometers were numbered as #1, #2, #3 and #4 in counterclockwise order, the exact placements of the four MEMS accelerometers are represented in Fig. 7.

The input shaft speed was set as 2350 r/min, the braking torque of the test rig was kept stable as 50 Nm. The time domain dynamic responses of the ring gear were recorded by experiment and simulated by the proposed dynamic model. The Fast Fourier Transform (FFT) was applied on the vibration acceleration signals and the comparisons of the simulation and experiment spectra of ring gear is depicted as Fig. 8(a) and (b). The theoretical rotational frequency f_r of ring gear was 15.95 Hz, and the experimental value was 16.25 Hz. The deviation between them was acceptable due to the errors of frequency controller and accelerometer. The simulation and experimental values of meshing frequencies were 924.7 Hz and 928.7 Hz, respectively. The meshing frequency errors of experimental acceleration spectrum and simulated acceleration spectrum were less than 1%. Both the experimental and simulation results show great cohesions with each other, and this indicates the correctness of the proposed model to a certain extent.

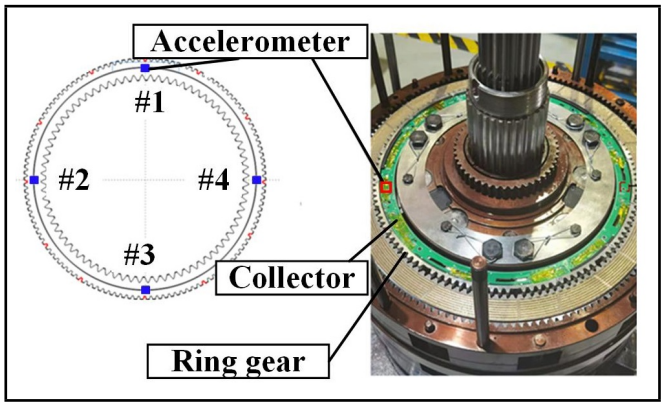

Figure 7. A test rig of the studied planetary gear transmission system.

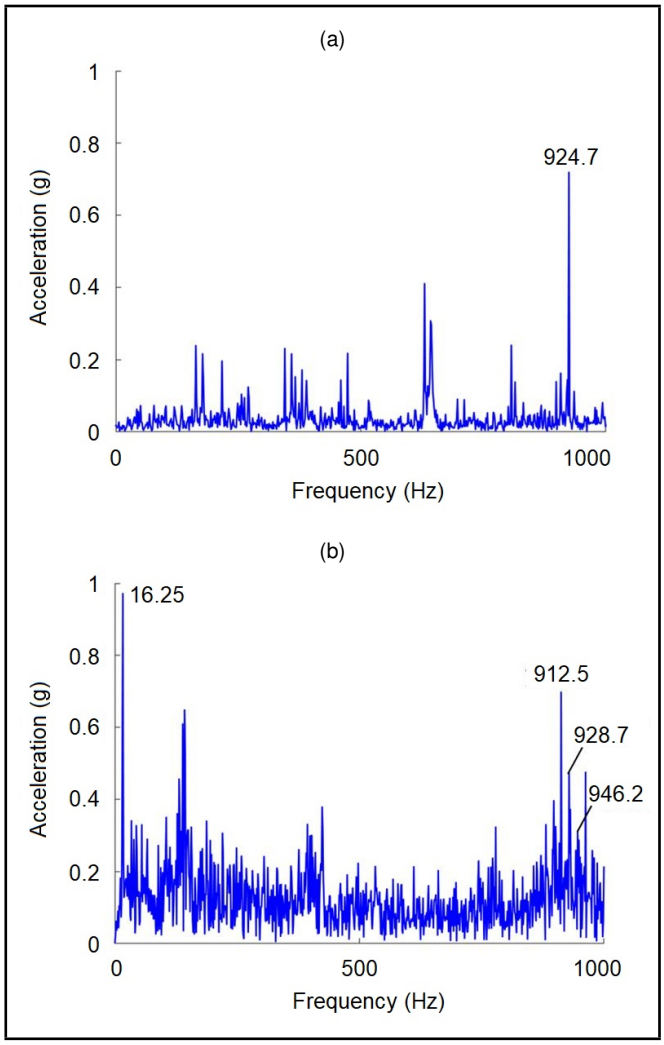

Figure 8. Comparison of simulation and experiment results. (a) Simulation spectrum, (b) experiment spectrum.

4. RESULTS AND DISCUSSION

The SODASRT 2 solver in Simpack is utilized for the solution. The time step was set as $\Delta t = 1 \times 10^{-5}$ s, the input speed and the output load of the SSPGS in each gear are set according to Table 5.

Table 4. Comparisons of frequencies for experimental and simulation results.

Frequencies	Theory value (Hz)	Experiment (Hz)	Simulation (Hz)
f_r	15.95	16.25	/
f_m	925.34	928.7	924.7

Table 5. Working conditions of the SSPGS.

Gear	Transmission ratio	Input speed (rad/s)	Output load (N·m)
F1	8.403	60.98	49073.93
F2	5.558	78.32	29026.29
F3	3.652	78.32	21712.09
F4	2.301	243.99	6059.68
F5	1.522	243.99	4008.19
F6	1	243.99	2633.5
R1	-5.969	-85.64	43637.71
R2	-4.191	-85.64	30287.103

Table 6. RMS values of angular accelerations for inner hubs in each gear (rad/s^2).

Gear	C1	C2	C3	CL	CR
F2	12972.05	0.00	5583.42	3132.83	2978.44
F3	3141.72	1742.04	1742.04	0.00	2593.60
F5	10243.49	0.00	7515.49	7751.92	0.00
F6	8309.98	4944.40	4944.40	7780.34	0.00
R2	6044.17	0.00	4855.89	4477.85	0.00

4.1. Vibration Characteristic of Clutch Inner Hub without Gear Godification

The RMS values of inner hub vibrations for different clutches in gears F2, F3, F5, F6 and R2 are shown in Fig. 9. The coordinates of the horizontal axis are corresponding to the inner hub for clutches C1, C2, C3, CL and CR, the bar graphs in five different colors are representing gears F2, F3, F5, F6 and R2. Because of the manipulators are changing in different gear, then the inner hubs that can vibrate are varies. For gear F2, the manipulators are C2 and CL, then the RMS values of inner hubs C1, CH and CR are obtained; for gear F3, the manipulators are C3 and CL, the vibration analyses can perform on the inner hubs C1, C2 and CR; for gear F5, the manipulators are C2 and CH, the vibration analyses are performed on the inner hubs C1, C3 and CL; for gear F6, the manipulators are C3 and CH, the vibration analyses are performed on the inner hubs C1, C2 and CL; for gear R2, the manipulators are C2 and CR, the vibration analyses are performed on the inner hubs of clutches C1 and CL.

Comparisons of inner hub angular accelerations around Z axis for different clutches in gears F2, F3, F5, F6 and R2 are shown in Fig. 9(a). As depicted in Fig. 9(a), the RMS values of angular accelerations around the Z axis of the inner hub C1 in gears F2 and F5 are significantly higher than those of the inner hubs of the other clutches. More details of the RMS values are plotted in Table 6. Comparisons of inner hub accelerations along X axis for different clutches are shown in Fig. 9(b). As depicted in Fig. 9(b), the RMS values of accelerations along the X axis of the inner hub C1 in gears F2 and F5 are also significantly higher than those of the other inner hubs. More details of the RMS values of accelerations along X axis are plotted in Table 7.

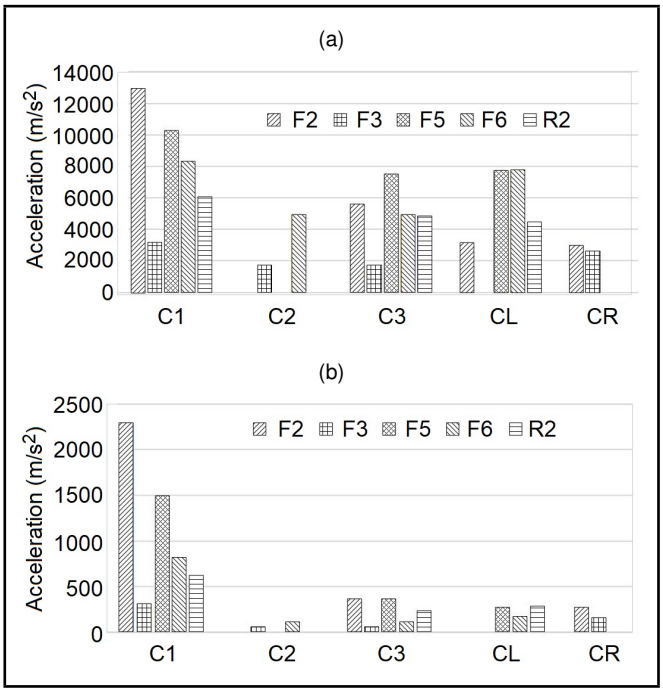

Figure 9. Comparisons of inner hub vibrations in different gear. (a) RMS values of angular acceleration around Z axis, (b) RMS values of accelerations along X axis.

Table 7. RMS values of accelerations for inner hubs in each gear (m/s^2).

Gear	C1	C2	C3	CL	CR
F2	2296.36	0.00	365.48	0.00	271.01
F3	311.11	59.22	59.22	0.00	143.73
F5	1479.94	0.00	366.82	272.12	0.00
F6	812.19	115.12	115.12	172.60	0.00
R2	621.38	0.00	224.20	283.15	0.00

Table 8. Parameters of tip modification for the third-row planetary gears.

Components	r_{Ca} (mm)	C_a (μm)
Long planetary gear	45.378	0, 10, 20, 30, 40, 50, 60, 70, 80, 90, 100
Short planetary gear	47.387	
Sun gear	72.187	

4.2. Vibration Characteristic of Clutch Inner Hub with Gear Modification

Results in Section 4.1 show that the vibrations of inner hub for clutch C1 is the most significant. To investigate the effects of gear tooth profile modification on the vibration suppression of the inner hub C1, the tooth profiles of the third-row planetary gears are modified. The maximum amounts of tip and flank modifications are defined in some existing standards such as British Standard (BS 1970) and ISO (ISO/DIS 1983), and the suggested maximum magnitude of modification is given.[23] According to these standards, the parameters of tip modification are plotted in Table 8.

For the gears F2 and F5, the vibrations of inner hub C1 under different tip modification amounts Ca are simulated and plotted in Figs. 10 and 11. Figure 10 shows the change trends of vibrations with modification amounts in gear F2. As shown in Fig. 10(a) and (c), the RMS values of angular accelerations around Z axis and accelerations along X axis both significantly decreases with the increase of modification amounts and the decreasing trends are quite uniform. While the PTP values of

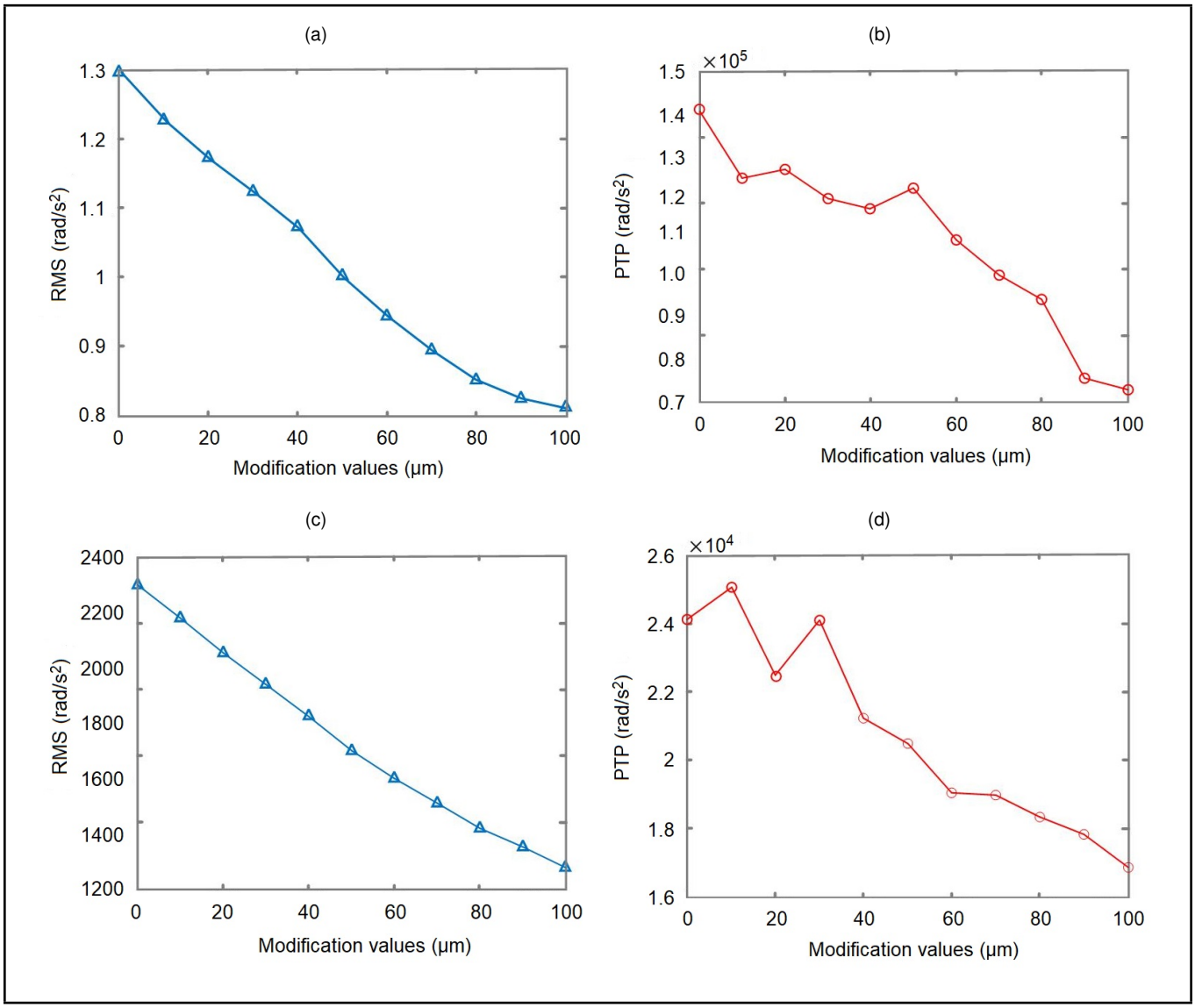

Figure 10. Effects of tip modification on the vibrations of inner hub C1 in gear F2. (a) RMS values of angular accelerations around Z axis, (b) PTP values of accelerations around Z axis, (c) RMS values of accelerations around X axis, (d) PTP values of accelerations along X axis.

those accelerations fluctuate with the increase of modification amounts and significant decrement can be observed.

Figure 11 shows the change trends of vibrations with modification amounts in gear F5. As shown in Fig. 11(a) and (c), in the range of $0 < C_a \leq 40$ μm, the modification amounts have more great influences on the RMS values of angular vibrations for inner hub C1. The RMS values of angular accelerations around Z axis significantly decrease from around 10200 rad/s^2 to 9000 rad/s^2 with the increase of modification amounts. While the RMS values of accelerations along X axis slightly decrease from 1480 m/s^2 to 1390 m/s^2. When the modification amount $C_a > 40$ μm, the RMS values of angular accelerations around Z axis and accelerations along X axis fluctuate with the increase of modification amounts and no apparent changing trends can be observed. The PTP values of those accelerations significantly fluctuate with the increase of modification amounts, as shown in Fig. 11(b) and (d). As depicted in Fig. 11(b) and (d), the PTP values decrease first then increase with the steady increase of modification amounts. And the PTP values of accelerations along X axis reach a peak when modification amount $C_a = 50$ μm.

5. CONCLUSIONS

In this study, the multibody dynamic model of a SSPGS is established by Simpack. The motion states of the components are specified with the joints. The engagement forces between meshing gear pairs and dynamic contact load between friction plates and inner hub of clutches are all considered by force elements. The dynamic model of the SSPGS is calculated and the inner hub of maximum vibration is located. The tip modification is introduced to suppress the vibration of inner hub and the effects of gear tooth modification on the vibrations of inner hub are investigated. Some conclusions are obtained:

(1) The inner hub of clutch C1 is identified as the inner hub of maximum vibration. The RMS values of angular accelerations and accelerations of the inner hub C1 in gears F2 and F5 are significantly higher than those of the inner hubs of the other clutches. Then the friction plate of inner hub C1 is most likely to break and vibration of inner hub C1 should be first suppressed.

(2) The tooth profile modification has more great influences

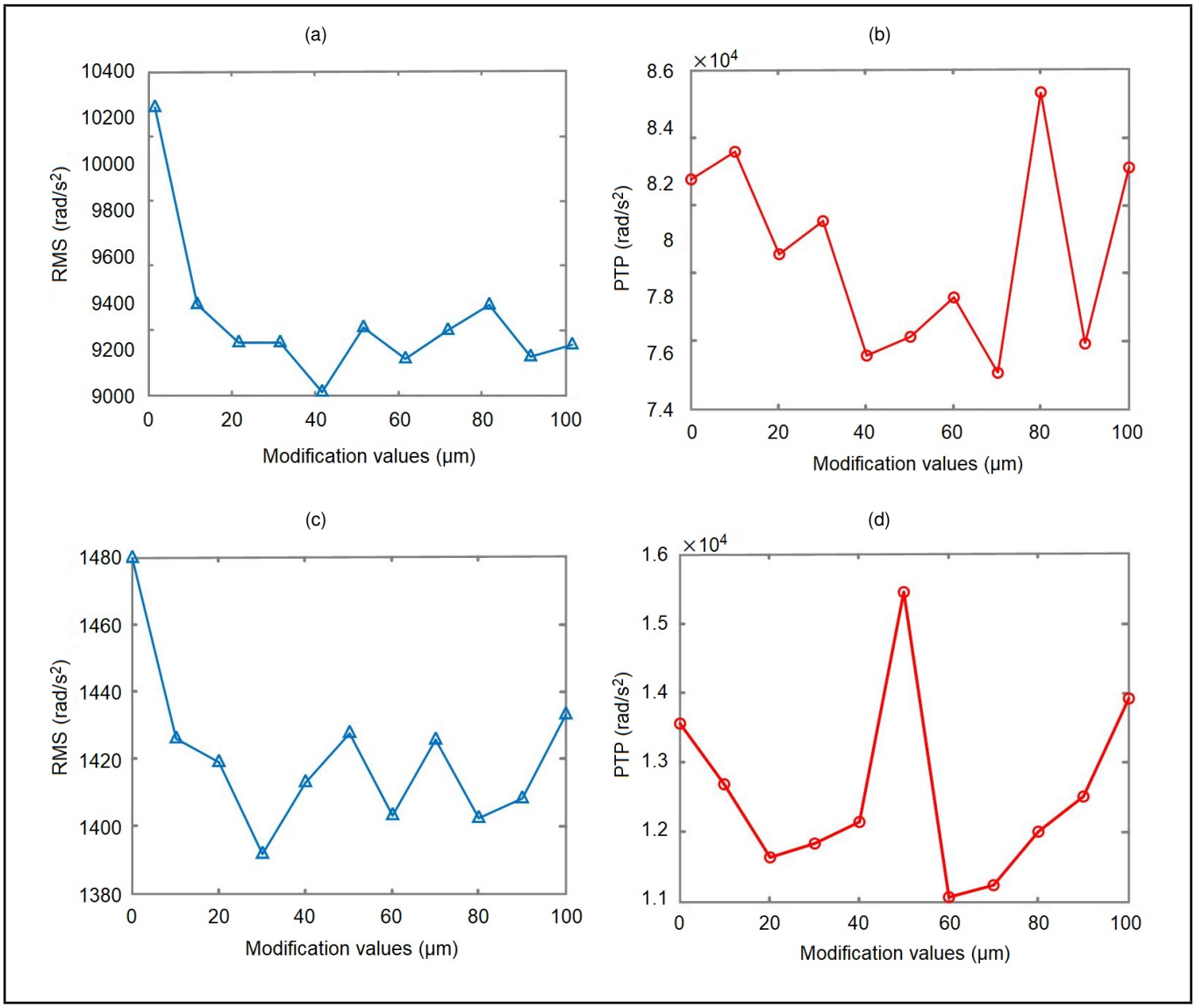

Figure 11. Effects of tip modification on the vibrations of inner hub C1 in gear F5. (a) RMS values of angular accelerations around Z axis, (b) PTP values of accelerations around Z axis, (c) RMS values of accelerations along X axis, (d) PTP values of accelerations along X axis.

on the angular vibrations than the lateral vibrations of inner hub C1. The angular accelerations significantly decrease from around 10200 rad/s^2 to 9000 rad/s^2 while the acceleration along X axis slightly change with the steady increase of modification amounts.

(3) Moderate tooth profile modification can suppress the vibrations of inner hub for SSPGS. The most optimum range of modification amount is identified as $0 < C_a \leq 40$ μm.

REFERENCES

[1] Zhang, C., Yu, W., Fan, C., Kong, C., Xu, J., and Shao, Y. Theoretical and experimental investigation on teeth impacts between the inner hub and the friction plate of the planetary transmission system's clutch, *Journal of Sound and Vibration*, **553**, 117674, (2023). https://doi.org/10.1016/j.jsv.2023.117674

[2] Chen, Q., Xu, R., Wang, Z., Pan, J., Huang, W., Zhang, J., and Wang, J. Analysis of electromechanical coupling vibration characteristics of motor-gear system based on bond graph theory, *AIP Advances*, **14** (1), 015315, (2024). https://doi.org/10.1063/5.0185079

[3] Li, S. and Zhou, S. A dynamic investigation of the impact failure analysis of the friction plate in a planetary transmission system, *International Journal of Acoustics and Vibration*, **25** (4), 577–586, (2020). https://doi.org/10.20855/ijav.2020.25.41716

[4] Liu, Y., Zhang, M., Lai, J., Li, H., Xu, J., Xu, X., and Song, X. Dynamic characteristics of the floating non-loaded ring gear with external spline teeth in Ravigneaux planetary gear sets, *Engineering Failure Analysis*, **142**, 106726, (2022). https://doi.org/10.1016/j.engfailanal.2022.106726

[5] Pan, W., Lan, H., Wang, L., Wang, B., Yang, L., and Shao, Y. Dynamic modeling for hydraulic disk brake with floating supported friction plate considering nonlinear tooth clearance impact, *Nonlinear Dynamics*, **111**, 18911-18930, (2023). https://doi.org/10.1007/s11071-023-08898-6

[6] Zhu, C., Chen, Z., Shi, Z., and Zhang, Y. Study on the engagement characteristics and control strategy of high speed difference dry friction clutch, *Machines*, **11** (3), 407, (2023). https://doi.org/10.3390/machines11030407

[7] Zhang, L., Wei, C., Hu, J., and Hu, Q. Nonlinear dynamic characteristics of rub-impact process at high circumferential velocities in no-load multiplate wet clutch, *Tribology Transactions*, **63** (1), 101–119, (2020). https://doi.org/10.1080/10402004.2019.1664685

[8] Yang, Y., Wang, Z., and Wang, Y. Thermoelastic coupling vibration and stability analysis of rotating circular plate in friction clutch, *Journal of Low Frequency Noise, Vibration and Active Control*, **38** (2), 558–573, (2019). https://doi.org/10.1177/1461348418817465

[9] Qu, J., Shi, W., Wang, J., and Chen, Z. Modeling and analysis of clutch nonlinear behavior in an automotive driveline for suppressing torsional vibration, *Machines*, **10** (9), 819, (2022). https://doi.org/10.3390/machines10090819

[10] Bao, H., Li, X., and Huang, W. Calculation method of radial displacement in the engaging process of wet friction clutch, *Journal of Mechanical Science and Technology*, **35**, 3909–3918, (2021). https://doi.org/10.1007/s12206-021-0804-9

[11] Ning, K., Wang, Y., Huang, D., and Yin, L. Impacting load control of floating supported friction plate and its experimental verification, *Journal of Physics: Conference Series*, **842** (1), 012070, (2017). https://doi.org/10.1088/1742-6596/842/1/012070

[12] Öztürk, V. Y., Cigeroglu, E., and Özgüven, H. N. Ideal tooth profile modifications for improving nonlinear dynamic response of planetary gear trains, *Journal of Sound and Vibration*, **500**, 116007, (2021). https://doi.org/10.1016/j.jsv.2021.116007

[13] Ni, H., Liu, J., Liu, D., Cao, H., and Pan, G. A novel dual deformation mode honeycomb sandwich cylindrical shell for enhanced stiffness and circumferential vibration isolation, *Mechanical Systems and Signal Processing*, **226**, 112359, (2025). https://doi.org/10.1016/j.ymssp.2025.112359

[14] Liu, J., Li, X., Pang, R., and Xia, M. Dynamic modeling and vibration analysis of a flexible gear transmission system, *Mechanical Systems and Signal Processing*, **197**, 110367, (2023). https://doi.org/10.1016/j.ymssp.2023.110367

[15] Liu, J., Li, X., and Xia, M. A dynamic model for the planetary bearings in a double planetary gear set, *Mechanical Systems and Signal Processing*, **194**, 110257, (2023). https://doi.org/10.1016/j.ymssp.2023.110257

[16] Li, X., Liu, J., Xu, J., Chen, Y., Hu, Z., and Pan, G. A vibration model of a planetary bearing system considering the time-varying wear, *Nonlinear Dynamics*, **111**, 19817-19840, (2023). https://doi.org/10.1007/s11071-023-08845-5

[17] Gao, P., Liu, H., Yan, P., Xie, Y., Xiang, C., and Wang, C. Research on application of dynamic optimization modification for an involute spur gear in a fixed-shaft gear transmission system, *Mechanical Systems and Signal Processing*, **181**, 109530, (2022). https://doi.org/10.1016/j.ymssp.2022.109530

[18] Huangfu, Y., Zhao, Z., Ma, H., Han, H., and Chen, K. Effects of tooth modifications on the dynamic characteristics of thin-rimmed gears under surface wear, *Mechanism and Machine Theory*, **150**, 103870, (2020). https://doi.org/10.1016/j.mechmachtheory.2020.103870

[19] Xu, X., Fan, X., Diao, P., and Liu, H. An investigation on the influence of modification parameters on transmission characteristics of planetary gear system, *Journal of Mechanical Science and Technology*, **33**, 3105–3114, (2019). https://doi.org/10.1007/s12206-019-0605-6

[20] Li, X., Xu, Y., Liu, J., Liu, J., Pan, G., and Shi, Z. Dynamic modelling of a floating spline-coupling shaft system with parallel misalignment and tooth backlash, *Mechanical Systems and Signal Processing*, **226**, 112363, (2025). https://doi.org/10.1016/j.ymssp.2025.112363

[21] Li, X., Xu, Y., Liu, J., Zhang, Y., Liu, J., Pan, G., and Shi, Z. Vibration analysis of the propulsion shaft system considering dynamic misalignment in the outer ring, *Journal of Sound and Vibration*, **589**, 118612, (2024). https://doi.org/10.1016/j.jsv.2024.118612

[22] Xu, Y., Liu, J., Li, X., and Tang, C. An investigation of vibrations of a flexible rotor system with the unbalanced force and time-varying bearing force, *Chinese Journal of Mechanical Engineering*, **38**, 25, (2025). https://doi.org/10.1186/s10033-025-01186-x

[23] Chen, Z. and Shao, Y. Mesh stiffness calculation of a spur gear pair with tooth profile modification and tooth root crack, *Mechanism and Machine Theory*, **62**, 63-74, (2013). https://doi.org/10.1016/j.mechmachtheory.2012.10.012